

A New Design of Large-format Streak Tube with Single-lens Focusing System

Liping Tian^{1,2}, Lingbin Shen¹, Lin Chen¹, Lili Li², Jinshou Tian², Ping Chen², Wei Zhao²

¹*School of network and communication engineering, Jinling Institute of Technology, Hongjing Road, No.99, Nanjing 211169, China, LB_shen@jit.edu.cn (L. Shen), chenlin@jit.edu.cn (L. Chen)*

²*Key Laboratory of Transient Optics and Photonics, Key Laboratory of Ultra-fast Photoelectric Diagnostics Technology, Xi'an Institute of Optics and Precision Mechanics, Chinese Academy of Sciences, Xixi Road, No.17, Xi'an, 710119, China*

Streak tubes with large-format and high spatial resolution are central to mm-spatial-resolved STIL detection system and hyperspectral resolved ICF experiment. In this paper, we established a large-format streak tube with a three-coaxial-cylindrical single-lens focusing system, a spherically curved photocathode and phosphor screen model in CST Particle Studio. The temporal and spatial resolution were calculated and mimicked based on the Monte-Carlo sampling method in static and dynamic mode. The simulated results show that the static spatial resolution reaches 50 lp/mm over the whole 50 mm effective photocathode length, and the physical temporal resolution is better than 45 ps. Furthermore, in dynamic working mode, the streak tube can achieve spatial resolution of 10 lp/mm and temporal resolution of 60 ps. The simulation results will be used to guide the design and production for large-format with high spatial resolution streak tube development.

Keywords: Ultrafast detector; Streak tube; single-lens focusing system; large format.

1. INTRODUCTION

Streak tube is a kind of photodevice consisting of a photocathode, a focusing electrode, a pair of deflection plates, an anode, and a phosphor screen. Due to ultra-high temporal resolution and high spatial resolution, the streak tube has been widely used in basic frontier scientific research and major original innovations, such as streak tube imaging lidar (STIL), inertial confinement fusion (ICF) diagnosis, (National Ignition Facility) NIF diagnosis detection, etc. [1]-[4]. However, the aberration of the electro-optical system of the streak tube, especially the increase of spherical aberration and distortion at the edge, limits the improvement of the effective photocathode and spatial resolution [5]-[7]. Over the past few decades, different approaches have been proposed and adopted to improve the spatial resolution of the streak tube and increase the effective photocathode working area. Improvement of the spatial resolution and working area of the streak tubes, however, has made little progress. To date, most large-format streak tubes adopt the curved photocathode and screen with the immersion-lens for focusing electrons [4], [8]-[11].

To solve the problem, we explored a promising single-lens focusing system which consists of three coaxial cylindrical electrodes with the same diameter instead of the traditional

immersion lens, combining the spherically curved photocathode and screen to improve the spatial resolution and enlarge the effective photocathode. Additionally, the difference between single-lens and an immersion lens is that the former is easier to use the voltage and focus electrons. The spherical photocathode and spherical phosphor screen technology can reduce aberrations, especially the edge aberrations of the electron optical system, and increase the detection area.

This paper describes the work performed in developing this streak tube with single-lens focusing system to obtain reliable evaluation, to achieve a spatial resolution higher than 40 lp/mm and MTF = 10 % over the entire effective photocathode of 50 mm, and to obtain a temporal resolution of less than 60 ps. This would be the most important step in the development of streak tube with a large-format and high spatial resolution. Moreover, other main characteristics of the streak tube, temporal resolution, static and dynamic spatial modulation transfer function, and dynamic scanning slit image have been evaluated, respectively.

2. 3D MODEL & METHODS

A schematic diagram of the large-format streak tube designed in this work is shown in Fig.1.a). There are a spherical photocathode and screen, a single-lens focusing

electrode, a pair of sweep plates, and an anode. This streak tube with a compact structure has the length of only 200 mm and the outer diameter of the tube is 90 mm. Spherical photocathode and screen are used for improving the spatial resolution, especially at the edge, thereby enlarging the photocathode effective working area by reducing the aberration of the electron optical system. In view of the good focusing performances of the single-lens, no matter whether the potential of the middle electrode is higher than the potential on both sides or lower than that, the single-lens can play a role of converging the electron beam. Thus, a single-lens is used as a focusing system to help improve the spatial resolution of the streak tube. All components, except for the fluorescent screen, are replaced by perfect electric conductor (PEC) materials when modeled in Computer Simulation Technology (CST), and the screen is replaced by a vacuum material to monitor the electron trajectory, counting the horizontal distribution of the electrons. Fig.1.b) shows the axial electric field distribution at different distances from the axis inside the streak tube calculated by the finite integration technique (FIT) method after applying voltage to each electrode, where r is the off-axis distance. In the streak tube, the electric field is always negative from the photocathode to the phosphor screen. Thus, the electrons emitted from the cathode are always accelerated. Whether on or off-axis, the axial electric field of the streak tube increases first in the negative direction and then decreases in the axis direction. The electric field reaches the maximum in the region from the focusing electrode to the anode. The farther away the electrons from the axis are in the region from the photocathode to the single-lens focusing electrode, the smaller the axial electric field is received, but the change is small. When the electrons emitted at different initial heights travel near the anode hole, almost all electrons move close to the axis. Additionally, the electric field experienced is mainly over the range of $r = 0 - 5$ mm. It can also be explained that the axis electric field at different distances from the axis affects the corresponding electrons. The operating speed of the machine has a certain impact, but the impact is small.

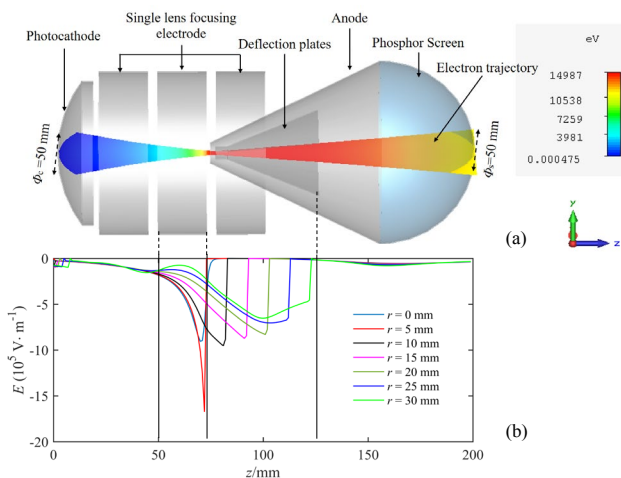


Fig.1. Schematic of the large-format streak tube and the electric field distribution.

The state of the electrons emitted from the photocathode is essential for evaluating the performance of the streak tube. Inspired by previous research, Monte-Carlo sampling method as a relatively mature electron emission model is adopted in our simulation. i. The initial energy of the electrons obeys the β distribution of 0-0.6 eV. ii. The launch elevation angle of the electrons obeys cosine distribution of 0~90 degrees. iii. The azimuth of the electrons obeys the uniform distribution of 0~ 2π . iv. It should be noted that the above parameters are fully independent of each other [12].

3. RESULTS

A. Static characteristics of spatiotemporal resolution

The physical temporal resolution of the streak tube is known as the amplification effect of the photoelectrons on the time scale when the photoelectrons move from the center of the photocathode to the phosphor screen without considering the scanning deflection electrostatic field [13]-[14]. Its essence attributes to the spread of the initial energy, the initial launch elevation angle and the initial azimuth of the electrons emitted from the photocathode. Here, the temporal modulation transfer function (TMTF) is adopted to calculate the temporal resolution. Fig.2. shows a limit physical SMTF of this streak tube. Temporal resolution, which is defined as the TMTF of this streak tube reduced to 0.1, is 43.6 ps. Fig.3. shows the simulation results of the physical temporal resolution of this streak tube. It suggests that the off-axis distance has little impact on the temporal resolution.

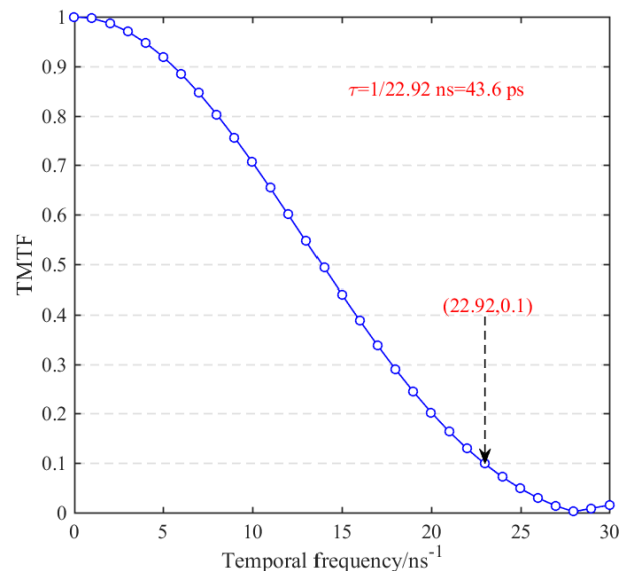


Fig.2. TMTF of this streak tube.

The spherical structure of the photocathode and the phosphor screen can minimize but not eliminate the adverse effects of temporal and spatial distortion. Research shows that the temporal distortion of the electronic optical system will bend the slit sweeping image [6]. The influence of the off-axis distance on its temporal distortion is investigated by

emitting photoelectrons with the same initial most probable energy of 0.15 eV from different initial heights of the photocathode. The temporal distortion for different positions of the photocathode is represented in Fig.4. As the off-axis distance increases, the temporal distortion of the streak tube also increases, except at 30 mm distance from the center. Affected by the edge electric field of the single-lens focusing electrode, the temporal distortion is reduced to -9 ps at a position of 30 mm off-axis. It is evident that the sweeping image would be a pillow-shaped deformation that decreases to negative temporal distortion in the range of the photocathode $\Phi 50$ mm.

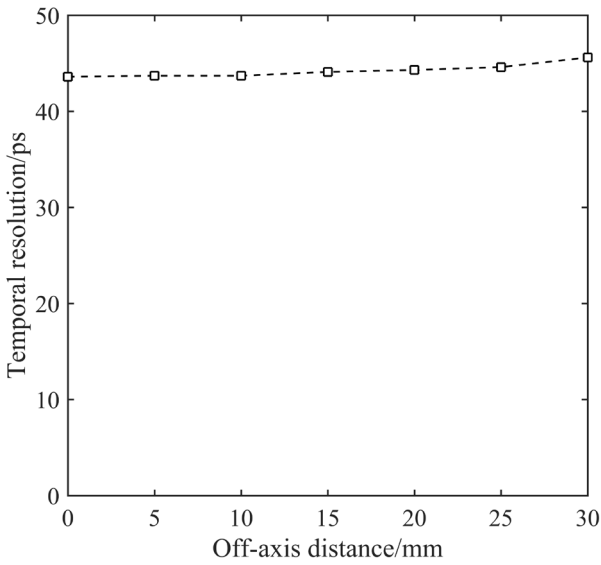


Fig.3. Physical temporal resolution of this streak tube.

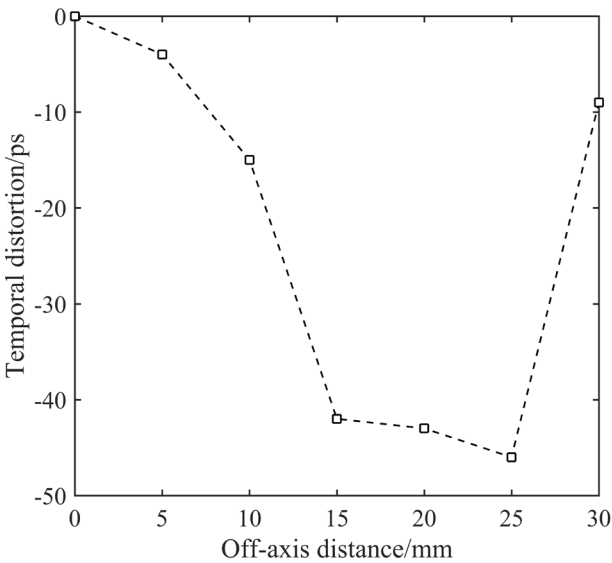


Fig.4. Temporal distortion of the streak tube.

For the positions outside the optical axis, due to the anisotropic electric field, the electron beam formed by the

electrons emitted from the photocathode surface is no longer rotationally symmetrical. Therefore, to fully evaluate the static spatial performance of the streak tube, we adopt the spatial modulation transfer function (SMTF) to calculate the spatial resolution. The spatial resolution is defined as the spatial frequency corresponding to the SMTF reduced to 0.1. Fig.5. exhibits the SMTF of this streak tube in sagittal direction for different off-axis distances. It is evident that off-axis distance has a marked effect on the spatial resolution. As mentioned above, with the increasing x , the spatial resolution decreases, which results in the aberration of the photocathode outer increase. In this simulation, the spatial resolution of this streak tube is higher than 50 lp/mm over the whole effective photocathode area of $\Phi 50$ mm.

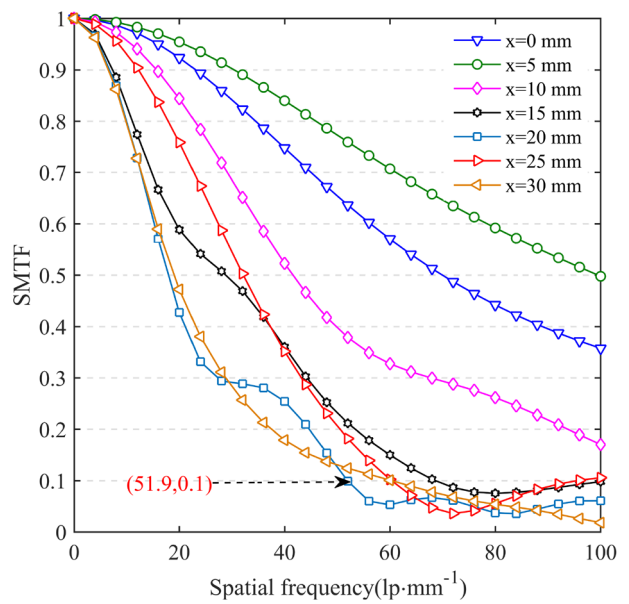


Fig.5. SMTF of the streak tube in sagittal direction.

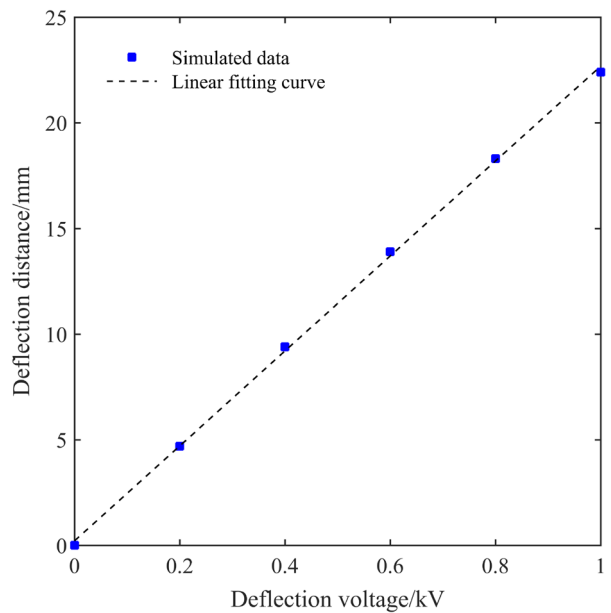


Fig.6. Relation between deflection distance and deflection voltage.

To restore the original image without distortion, the offset of the electrons emitted from the photocathode on the phosphor screen should be in a linear relationship with the voltage. Fig.6. shows the deflection linearity obtained by using the trajectory tracking method under different deflection voltages from 100 V to 800 V by step of 100 V. Obviously, the streak tube has good deflection linearity. The relationship between the deflection distance and the deflection voltage is obtained by polynomial fitting as equation (1).

$$y=22.47 x+0.214 \quad (1)$$

Where y is the deflection distance, x is the deflection voltage. Thus, we can conclude that the deflection sensitivity of this streak tube is 22.5 mm/kV.

B. Dynamic characteristics of spatiotemporal resolution

The temporal resolution of the streak tube is limited by the physical temporal spread and technical temporal spread. The latter comes mainly from the deflection sweeping speed, finite static image size and space charge effect among electrons [13]. In our simulation, the effects of the space charge effect are not taken into account. The static image size is 10 μm according to the static spatial resolution. Two consecutive electron pulses, δ_1 and δ_2 , with interval of 60 ps and full width at half maxima (FWHM) of 1 ps are emitted from the photocathode, as shown in Fig.7. The time for photoelectrons to enter the deflection system is around $t_1=4100$ ps, and the time to exit the deflection system is around $t_2= 5100$ ps. Considering that the linearity of the scanning system affects the imaging quality, the time window for applying the scanning voltage is over the range of 3600 ps to 5600 ps to make full use of photoelectron scanning in the linear region. The sweeping speed of the streak tube is set to be 2.3×10^7 m/s, and the corresponding ramp voltage is shown in Fig.8.

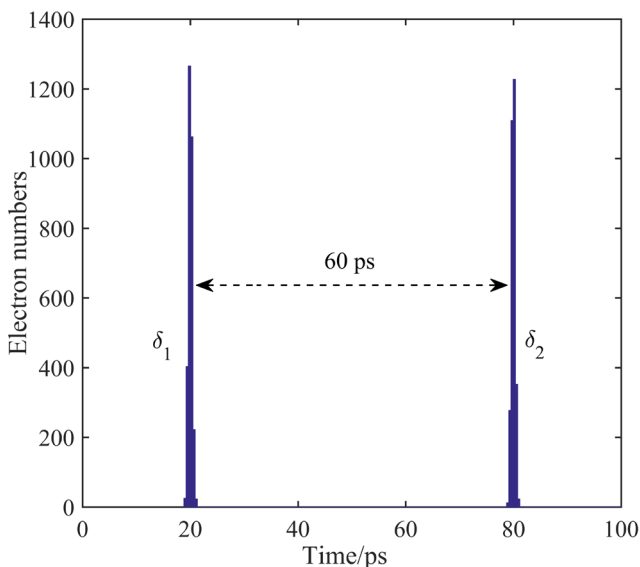


Fig.7. Two electron pulses with time interval of 60 ps

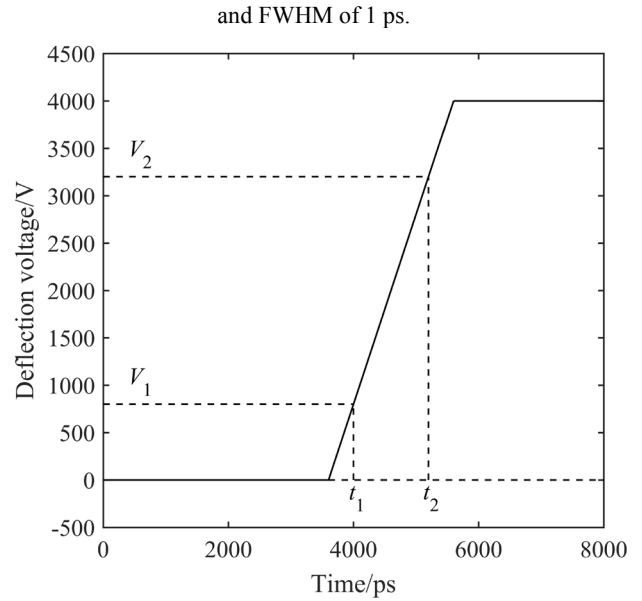


Fig.8. Swept voltage on the deflection plates.

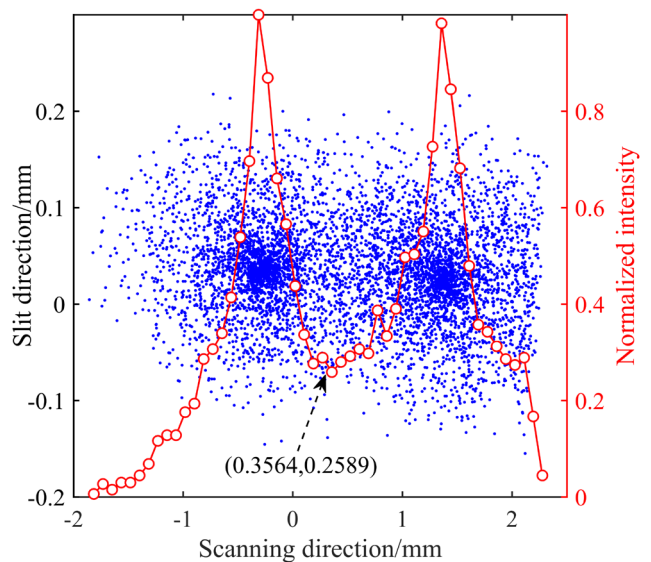


Fig.9. Electron distribution on the screen and normalized intensity in meridian direction.

Affected by the effect of temporal and spatial spread, the electron pulse distribution reaching the phosphor screen has also dispersion in both time and space axis. Fig.9. shows the distribution of the scanning electron pulses on the phosphor screen and the normalized distribution curve along the sagittal direction. It is evident that both electron pulses partially overlap when they reach the phosphor screen. However, the red line shows that the distribution probability corresponding to the valley bottom position of probability distribution curve in the meridian direction is lower than 0.7, required by the Rayleigh criterion. Therefore, the temporal resolution of this streak tube is better than 60 ps, due to the electron pulses an interval of 60 ps can be distinguished.

In the dynamic working mode, the spatial resolution in sagittal direction indicates the spatial dispersion, while the

spatial resolution in meridian direction shows both the temporal and spatial dispersion of the streak tube. Therefore, the spatial resolution in sagittal direction is calculated to characterize the spatial dispersion of the streak tube, as shown in Fig.10. It is evident that the spatial resolution is better than 10 lp/mm, even 25 mm off-axis. It can be easily understood that the effective photocathode area will be larger than 50 mm.

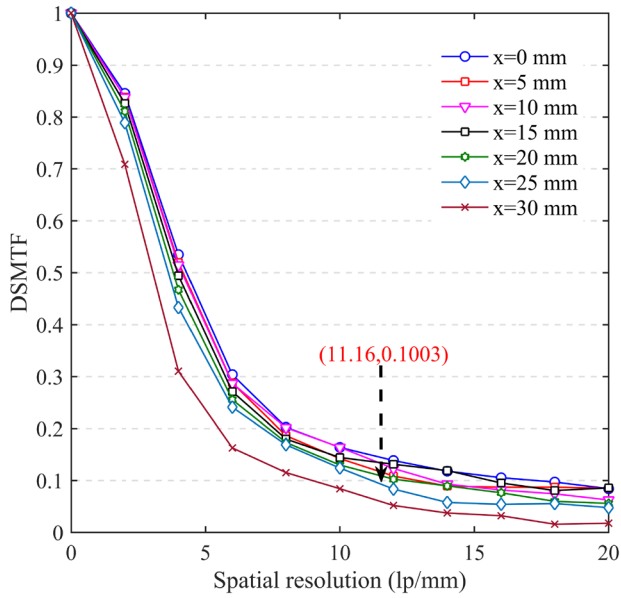


Fig.10. Dynamic SMTF of the streak tube in sagittal direction.

C. Multiple-slit imaging performance

For a streak tube with large effective photocathode area, the temporal distortion should be larger. Slits with a length of 36 mm, which is the embedded square of the photocathode, and a width of $50 \mu\text{m}$ are selected for multi-slit dynamic simulation of this streak tube. Nineteen electron pulses with Gaussian temporal distribution and a certain spatial interval are emitted from the photocathode inner surface, as shown in Fig.11.a). In the same way, the electron emission position obeys uniform distribution. The slope of the scanning signal applied to the deflection plates is $0.15 c$.

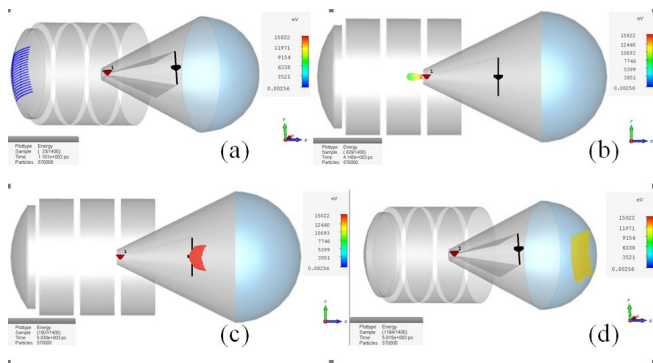


Fig. 11. Trajectories of multi-slit electrons at the different instant time.

Fig.11.a)~Fig.11.d) shows the evolution of multi-slit photoelectrons in this streak tube. Fig.12. shows the sweeping slit image of this streak tube. Obviously, the slit images have clear boundaries and no overlap at all. However, the multi-slit image bends downwards, mainly due to negative temporal distortion of the streak tube.

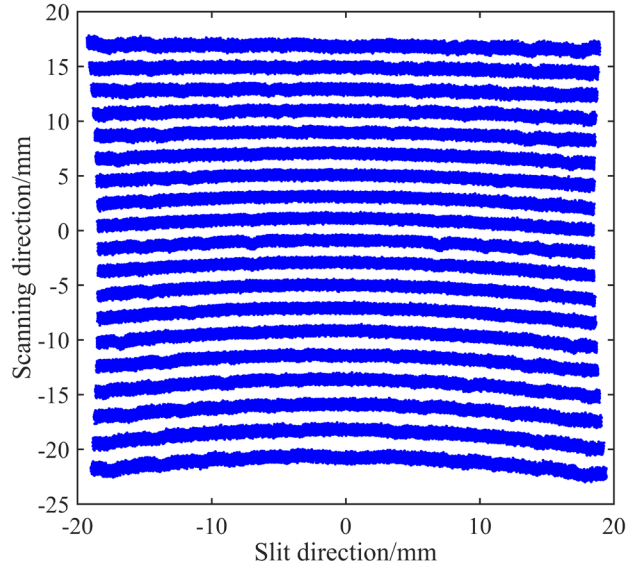


Fig.12. Sweeping image of the multi-slit electron pulses.

4. CONCLUSIONS

In this paper, a large-format and high spatio-temporal resolution streak tube suitable for the STIL detection system and ICF experiment is presented. The streak tube adopts a three-coaxial-cylindrical single-lens focusing system, instead of traditional immerse focusing lens, to improve voltage adjustability and focusing performance. A spherically curved photocathode and phosphor screen are used to reduce the image curvature and aberrations, thereby helping to achieve a high spatial resolution. The performances of the large-format streak tube were numerically investigated by using the FIT and M-C methods. The simulated physical temporal resolution is around 45 ps, for spherical curved structure, which is barely no difference at all in different off-axis distances. The static spatial resolution decreases as the off-axis distance increases, and then, it is still higher than 50 lp/mm at edge of $x=25 \text{ mm}$. In dynamic working mode, the trajectory of the electrons was monitored in PIC. Furthermore, the temporal resolution of 60 ps is obtained by using the Rayleigh criterion. When scanning speed is $0.15 c$, the dynamic spatial resolution can reach 10 lp/mm over the whole 50 mm effective photocathode length.

Table 1. Performance parameters of this streak tube.

Parameters	This streak tube
1 Photocathode effective area (mm)	$\geq\Phi 50$
2 Physical temporal resolution (ps)	<60
3 Static spatial resolution at the photocathode (lp/mm)	≥ 40
4 Electro-optical magnification	≈ 1
5 Deflection sensitivity (mm/kV)	22.47
6 Phosphor screen area (mm)	$\Phi 50$
7 Dynamic spatial resolution (lp/mm)	≥ 10
8 Working voltage (kV)	15
9 External dimensions (mm \times mm)	$<\Phi 90 \times 200$

ACKNOWLEDGMENT

This study is supported by Scientific Instrument Developing Project of the Chinese Academy of Sciences (Grant No. GJJSTD20190004), the Nature Science Foundation of Jiangsu Province, China (Grant No. BK20190112), the Open Research Fund of State Key Laboratory of Transient Optics and Photonics (Grant No. SKLST202012), and the Ph.D. Project supported by the Jinling Institute of Technology (Grant No. jit-b-201814 and No. jit-b-202012).

REFERENCES

- [1] Xia, W., Han, S., Ullah, N., Cao, J., Wang, L., Cao, J., Cheng, Y., Yu, H. (2017). Design and modeling of three-dimensional laser imaging system based on streak tube. *Applied Optics*, 56 (3), 487-497.
- [2] Ye, G., Fan, R., Lu, W., Dong, Z., Li, X., He, P., Chen, D. (2016). Depth resolution improvement of streak tube imaging lidar using optimal signal width. *Optical Engineering*, 55 (10), 103112.
- [3] Macphee, A.G., Dymoke-Bradshaw, A., Hares, J.D., et al. (2016). Improving the off-axis spatial resolution and dynamic range of the NIF X-ray streak cameras (invited). *Review of Scientific Instruments*, 87 (11), 420-568.
- [4] Howorth, J.R., Milnes, J.S., Fisher, Y., Jadwin, A., Boni, R., Jaanimagi, P.A. (2016). The development of an improved streak tube for fusion diagnostics. *Review of Scientific Instruments*, 87 (11), 287-294.
- [5] Shchelev, M.Y., Andreev, S.V., Greenfield, D.E., Degtyareva, V.P., Kopaev, I., Monastyrskiy, M. (2015). On some limitations on temporal resolution in imaging subpicosecond photoelectronics. *Quantum Electronics*, 45 (5), 455-461.
- [6] Hui, D., Tian, J., Lu, Y., Wang, J., Wen, W., Liang L., Chen, L. (2016). Temporal distortion analysis of the streak tube. *Acta Physica Sinica*, 65 (15), 158502.
- [7] Tian, L., Shen, L., Li, L., Wang, X., Chen, P., Wang, J., Chen, L., Zhao, W., Tian, J. (2021). Small-size streak tube with high edge spatial resolution. *Optik*, 242, 166791.
- [8] Hui, D., Luo, D., Tian, L., et al. (2018). A compact large-format streak tube for imaging lidar. *Review of Scientific Instrument*, 89 (4), 045113.
- [9] Tian, L.-P., Li, L.-L., Wen, W.-L., Wang, X., Chen, P., Lu, Y., Wang, J.-F., Zhao, W., Tian, J.-S. (2018). Numerical calculation and experimental study on the small-size streak tube. *Acta Physica Sinica*, 67 (18), 188501.
- [10] Ageeva, N.V., Andreev, S.V., Belolipetski, V.S., et al. (2009). Small-size meshless 50 ps streak tube. In *28th International Congress on High-speed Imaging and Photonics*. SPIE, 71260A.
- [11] Feldman, G.G., Jilkina, V.M., Razdobarin, G.T. (1998). PV-400 picosecond streak tube with large format photocathode. *Optical Engineering*, 37 (8), 2247-2248.
- [12] Tian, L.-P., Wen, W.-L., Wang, X., Chen, P., Hui, D.-D., Lu, Y., Tian, J.S., Zhao, W. (2019). Research on the spatio-temporal and gain performances on the small-size streak tube. *Acta Photonica Sinica*, 48 (7), 723002.
- [13] Feng, J., Shin, H.J., Nasiatka, J.R., et al. (2007). An x-ray streak camera with high spatio-temporal resolution. *Applied Physics Letters*, 91 (13), 134102.
- [14] Shakya, M.M., Chang, Z. (2005). Achieving 280 fs resolution with a streak camera by reducing the deflection dispersion. *Applied Physics Letters*, 87 (4), 111.

Received July 5, 2021
Accepted October 19, 2021